

Nanoscale Homochiral C_3 -Symmetric Mixed-Valence Manganese Cluster Complexes with Both Ferromagnetic and Ferroelectric Properties

Cai-Ming Liu,^{*,†} Ren-Gen Xiong,[‡] De-Qing Zhang,[†] and Dao-Ben Zhu[†]

Beijing National Laboratory for Molecular Sciences, Center for Molecular Science, Institute of Chemistry, Chinese Academy of Sciences, Beijing 100190, P. R. China, and Ordered Matter Science Research Center, Southeast University, Nanjing 211189, P. R. China

Received December 6, 2009; E-mail: cmliu@iccas.ac.cn

Nanoscale high-nuclear transition-metal cluster complexes have led to intense research interest because of their aesthetical structures and their rich electronic and magnetic properties that have potential applications in metalloenzyme models, single-molecule magnets, catalysts, and nanoelectronic components.¹ On the other hand, chirality can induce novel functions such as the magnetochiral dichroism (MChD) effect² and nonlinear optical³ and ferroelectric properties⁴ in magnetic molecules, generating multifunctional molecular materials, especially multiferroic materials, in which both ferromagnetic and ferroelectric properties coexist.⁵ However, only a few X-ray structurally characterized nanoscale chiral polynuclear cluster complexes are known,⁶ and the great difficulty is that most of chiral aggregates usually crystallize as racemic mixtures or undergo rapid racemization in solution.^{6a}

One strategy for assembling chiral multinuclear transition-metal magnetic clusters is using the *R* and *S* forms of the ligand, which causes the structures to crystallize in enantiomeric crystal forms. We sought to induce the ferroelectric property in chiral ferromagnetic high-nuclear transition-metal cluster complexes for the design of multiferroic molecule-based materials by utilizing two enantiomeric Schiff base ligands, *R*- and *S*-H₃L (Figure 1a), to construct the first nanoscale homochiral manganese cluster complexes with both ferroelectric and ferromagnetic properties: $\{[\text{Mn}^{\text{III}}_3\text{Mn}^{\text{II}}(\text{O})(\text{H}_2\text{O})_3(\text{R-L})_3]_4[\text{Mn}^{\text{III}}_6\text{Cl}_4\text{O}_4][\text{Mn}^{\text{III}}_3(\text{O})(\text{H}_2\text{O})_3(\text{R-L})_3](\text{OH})_4 \cdot 21\text{H}_2\text{O} \cdot 3\text{MeOH}$ (*R*-1) and $\{[\text{Mn}^{\text{III}}_3\text{Mn}^{\text{II}}(\text{O})(\text{H}_2\text{O})_3(\text{S-L})_3]_4[\text{Mn}^{\text{III}}_6\text{Cl}_4\text{O}_4][\text{Mn}^{\text{III}}_3(\text{O})(\text{H}_2\text{O})_3(\text{S-L})_3](\text{OH})_4 \cdot 21\text{H}_2\text{O} \cdot 3\text{MeOH}$ (*S*-1).

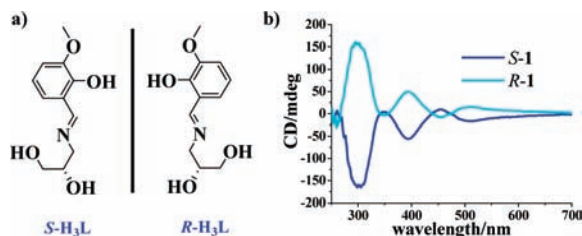


Figure 1. (a) Chiral Schiff bases *R*- and *S*-H₃L. (b) CD spectra of *R*-1 and *S*-1 at room temperature (2×10^{-5} M, MeOH).

The *R*-1 and *S*-1 enantiomers were prepared by the reactions of Schiff bases *R*- and *S*-H₃L, respectively, with MnCl₂ in the presence of Et₃N [see the Supporting Information (SI)]. Their circular dichroism (CD) spectra were measured to confirm their optical activity and enantiomeric nature. *R*-1 exhibited a strong positive Cotton effect at 300 nm and a positive dichroic signal centered at 394 nm, while *S*-1 showed Cotton effects of the opposite sign at

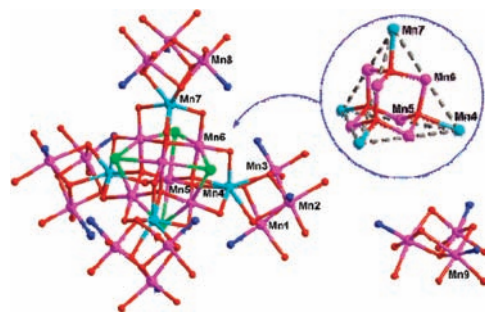


Figure 2. Cluster structures of *R*-1. C atoms have been omitted for clarity. Color code: Mn³⁺, purple; Mn²⁺, cyan; O, red; N, blue; Cl, green. Inset: the $[\text{Mn}^{\text{III}}_6\text{Mn}^{\text{II}}_4\text{O}_4]^{18+}$ supratetrahedral core of the cluster cation.

the same wavelengths (Figure 1b). These Cotton effect peaks can be assigned to the charge transfer transitions of the UV–vis absorption spectra (see the SI).

Single-crystal X-ray diffraction analyses revealed that *R*-1 and *S*-1 show C_3 -symmetric structures composed of a 22-nucleus manganese cluster cation, $\{[\text{Mn}^{\text{III}}_3\text{Mn}^{\text{II}}(\text{O})(\text{H}_2\text{O})_3\text{L}_3]_4[\text{Mn}^{\text{III}}_6\text{Cl}_4\text{O}_4]\}^{6+}$, and a trinuclear manganese cluster anion, $[\text{Mn}^{\text{III}}_3\text{O}(\text{H}_2\text{O})_3\text{L}_3]^{2-}$ (Figure 2; also see the SI). There are 15 chiral stereogenic centers from the 15 chiral Schiff bases. The manganese oxidation states were established by bond valence sum calculations (see the SI). The cluster cation comprises four $\text{Mn}^{\text{III}}_3\text{Mn}^{\text{II}}(\text{O})(\text{H}_2\text{O})_3\text{L}_3$ distorted cubane subunits that are linked around a $[\text{Mn}^{\text{III}}_6\text{Cl}_4\text{O}_4]^{6+}$ core via oxo bridges. The core consists of a Mn^{III}₆ distorted octahedron with one set of nonadjacent faces bridged by $\eta^3\text{-O}^{2-}$ anions and the other set of nonadjacent faces by $\eta^3\text{-Cl}^-$ anions. This core is also a near tetrahedron of Cl⁻ vertexes with a Mn³⁺ cation at the midpoint of each edge and an $\eta^3\text{-O}^{2-}$ anion bridging each face, which is similar to those in $\text{Mn}^{\text{III}}_6\text{X}_4\text{O}_4(\text{R}_2\text{dbm})_6$ [dbmH = dibenzoylmethane; X = Cl, Br; R = H, Me, Et].⁷ Each Mn³⁺ cation adopts a distorted octahedral geometry, with two coordinate sites occupied by two $\eta^4\text{-O}^{2-}$ anions shared with Mn²⁺ cations in the $\text{Mn}^{\text{III}}_3\text{Mn}^{\text{II}}(\text{O})(\text{H}_2\text{O})_3\text{L}_3$ distorted cubane subunits. There is a Jahn–Teller (JT) distortion, with a remarkable axial elongation of the two trans Mn–Cl bonds. Three identical $\text{Mn}^{\text{III}}_3\text{Mn}^{\text{II}}(\text{O})(\text{H}_2\text{O})_3\text{L}_3$ cubane subunits are symmetrically linked around the $[\text{Mn}^{\text{III}}_6\text{Cl}_4\text{O}_4]^{6+}$ core as a tripod and the fourth is at the zenith, generating a $[\text{Mn}^{\text{III}}_6\text{Mn}^{\text{II}}_4\text{O}_4]^{18+}$ supratetrahedron with Mn²⁺ ions at the vertexes, a Mn³⁺ ion lying along each edge, and four central tetrahedral $\eta^4\text{-O}^{2-}$ anions bridging the metal ions. This supratetrahedral arrangement is reminiscent of the structures of the Chevrel phases and similar to that of $[\text{Mn}^{\text{II}}_4\text{Mn}^{\text{III}}_6\text{Br}_4\text{O}_4(\text{amp})_6(\text{ampH}_2)_3(\text{HampH}_2)]\text{Br}_3 \cdot 8\text{hexane}$ (ampH₂ = 2-amino-2-methyl-1,3-propanediol).⁸ Although mixed-valence tetranuclear Mn compounds involving Schiff base ligands are well-known,⁹ this is the first example in which they are linked to a cluster core as subunits. The Mn³⁺ octahedral configuration in each cubane subunit is completed by a phenoxide O atom and an imino atom along with

[†] Institute of Chemistry.

[‡] Southeast University.

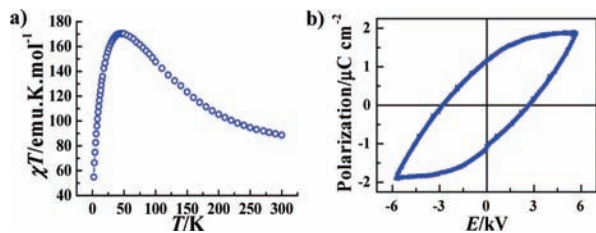


Figure 3. (a) Plot of χT versus T for *R*-1 measured under a field of 1 kOe. (b) Electric hysteresis loop for *R*-1 at room temperature, observed for a single-crystal sample using a ferroelectric tester.

an η^3 -alkoxide O atom from one L^{3-} , an η^3 - O^{2-} atom, an η^3 -alkoxide O atom from another L^{3-} , and a terminal H_2O molecule, which form the JT elongation axes. The Mn^{2+} cation is coordinated by three η^3 -alkoxide O atoms shared with the Mn^{3+} cations, three η^2 -alkoxide O atoms, and one η^4 - O^{2-} anion shared with the $[Mn^{III}_6Cl_4O_4]^{6+}$ core.

The $[Mn^{III}_3O(H_2O)_3L_3]^{2-}$ cluster anion features a $\{(Mn^{III})_3(\eta^3-O)\}^{7+}$ pyramidal unit with each edge bridged by one alkoxide O atom of an L^{3-} ligand, whose phenoxide O atom and imino atom are bound terminally but whose end alkoxide O atom is left free. The central O atom lies 1.14 Å above the plane of the Mn^{III} , equilateral triangle. The Mn^{3+} cation also adopts an octahedral configuration, coordinated by a phenoxide O atom and an imino atom along with an η^2 -alkoxide O atom from one L^{3-} , an η^3 - O^{2-} atom, an η^2 -alkoxide O atom from another L^{3-} , and a terminal H_2O molecule, which generate the JT elongation axes.

The thermal variation of χT for *R*-1 over the temperature range 2–300 K is shown in Figure 3a. The value of χT at room temperature is 88.62 emu K mol $^{-1}$, which is somewhat larger than the value expected for 21 magnetically isolated manganese(III) ions and four manganese(II) ions (80.5 emu K mol $^{-1}$ for $g = 2.0$). The χT product increases continuously to a maximum of 170.40 emu K mol $^{-1}$ at 46 K before dropping to 54.88 emu K mol $^{-1}$ at 2 K, suggesting dominating ferromagnetic interactions and a large ground-state spin value S_T . The decline in the χT value below 46 K is assigned to zero-field splitting, Zeeman effects, and/or intercluster interactions. Above 150 K, the χ^{-1} versus T plot obeys the Curie–Weiss law with $\Theta = 71.5$ K and $C = 71.4$ emu K mol $^{-1}$. The positive Θ value confirms that the ferromagnetic interaction is regnant.

The magnetization variation for *R*-1 at different applied fields was determined between 2 and 6 k (see the SI). The nonsuperposition of the isofield lines indicates the significant zero-field splitting, and the saturation $M/N\beta$ value of 42 suggests that $S_T \approx 20$, which is reasonable because (1) the $Mn^{3+} \cdots Mn^{3+}$ interactions within the $[Mn^{III}_6Cl_4O_4]^{6+}$ core,⁷ within the $[Mn^{III}_3O(H_2O)_3L_3]^{2-}$ cluster anion, and between the $[Mn^{III}_6Cl_4O_4]^{6+}$ core and the Mn^{2+} cations are expected to be ferromagnetically coupled and (2) the spin ground state of the $[Mn^{III}_3Mn^{II}(O)(H_2O)_3L_3]$ cubane subunit is $(5/2 + 2) - (2 \times 2) = 0.5$, which would give a total S_T of $(6 \times 2) + (3 \times 2) + (0.5 \times 4) = 20$. However, it was not possible to obtain a reasonable fit for these data using the ANISOFIT program.¹⁰ This is likely due to the intercluster exchange interactions, which are not incorporated in the fitting model. Down to 1.8 K, slow paramagnetic relaxation was not observed from ac susceptibility studies under a 2.5 Oe oscillating field at frequencies up to 997 Hz (see the SI).

Since *R*-1 and *S*-1 crystallize in chiral space group *R*3, which belongs to one of ten polar points (3), they should in principle have ferroelectric properties.^{4,11} The ferroelectric behavior of *R*-1 was examined at room temperature. Figure 3b clearly shows that there is an electric hysteresis loop with a remnant polarization (P_r) of 1.16 $\mu C cm^{-2}$ and a coercive field (E_c) of 2.65 kV cm $^{-2}$. The saturation value of the spontaneous polarization (P_s), $\sim 1.92 \mu C$

cm $^{-2}$, is much larger than that of the Rochelle salt ($P_s = 0.25 \mu C cm^{-2}$). The low-temperature (–180 to 0 °C) dependence of the ac dielectric permittivity measurements indicated that the frequency dielectric constant is strongly temperature-dependent: it increases continuously and ascends rapidly for $T > -100$ °C upon warming, reaching a value of 11.6 at 10 kHz and 0 °C (see the SI), confirming the ferroelectric property.

In conclusion, this work has demonstrated a promising approach to nanoscale multiferroic molecule-based materials that uses a strategy involving chiral Schiff base manganese clusters.

Acknowledgment. This work was supported by the National Natural Science Foundation of China (20473096 and 20671093), the 973 Program (2006CB932101), and CAS.

Supporting Information Available: Experimental details, supporting figures, and CIF files. This material is available free of charge via the Internet at <http://pubs.acs.org>.

References

- (1) (a) Gatteschi, D.; Sessoli, R.; Villain, J. *Molecular Nanomagnets*; Oxford University Press: New York, 2007. (b) Yoshizawa, M.; Tamura, M.; Fujita, M. *Science* **2006**, *312*, 251. (c) Holm, R. H.; Kennepohl, P.; Solomon, E. I. *Chem. Rev.* **1996**, *96*, 2239. (d) Bogani, L.; Wernsdorfer, W. *Nat. Mater.* **2008**, *7*, 179. (e) Christou, G.; Gatteschi, D.; Hendrickson, D. N.; Sessoli, R. *MRS Bull.* **2000**, *25*, 66. (f) Murugesu, M.; Habrych, M.; Wernsdorfer, W.; Abboud, K. A.; Christou, G. *J. Am. Chem. Soc.* **2004**, *126*, 4766. (g) Leuenberger, M. N.; Loss, D. *Nature* **2001**, *789*. (h) Newton, G. N.; Cooper, G. J. T.; Kögerler, P.; Long, D.-L.; Cronin, L. *J. Am. Chem. Soc.* **2008**, *130*, 790. (i) Wang, W.-G.; Zhou, A.-J.; Zhang, W.-X.; Tong, M.-L.; Chen, X.-M.; Nakano, M.; Beedle, C. C.; Hendrickson, D. N. *J. Am. Chem. Soc.* **2007**, *129*, 1014. (j) Liu, T.; Zhang, Y.-J.; Wang, Z.-M.; Gao, S. *J. Am. Chem. Soc.* **2008**, *130*, 10500. (k) Bi, Y.; Wang, X.-T.; Liao, W.; Wang, X.; Zhang, H.; Gao, S. *J. Am. Chem. Soc.* **2009**, *131*, 11650. (l) Lisnard, L.; Tuna, F.; Candini, A.; Affronte, M.; Wimpenny, R. E. P.; McInnes, E. J. L. *Angew. Chem., Int. Ed.* **2008**, *47*, 9695. (m) Zaleski, C. M.; Depperman, E. C.; Dendrinou-Samara, C.; Alexiou, M.; Kampf, J. W.; Kessissoglou, D. P.; Kirk, M. L.; Pecoraro, V. L. *J. Am. Chem. Soc.* **2005**, *127*, 12862.
- (2) Rikkin, G. L. J. A.; Raupach, E. *Nature* **1997**, *390*, 493.
- (3) (a) Bogani, L.; Cavigli, L.; Bernot, K.; Sessoli, R.; Gurioli, M.; Gatteschi, D. *J. Mater. Chem.* **2006**, *16*, 2587. (b) Train, C.; Nuida, T.; Gheorghie, R.; Gruselle, M.; Ohkoshi, S.-i. *J. Am. Chem. Soc.* **2009**, *131*, 16838.
- (4) (a) Fu, D.-W.; Song, Y.-M.; Wang, G.-X.; Ye, Q.; Xiong, R.-G.; Akutagawa, T.; Nakamura, T.; Chan, P. W. H.; Huang, S. D. *J. Am. Chem. Soc.* **2007**, *129*, 5346. (b) Gu, Z.-G.; Zhou, X.-H.; Jin, Y.-B.; Xiong, R.-G.; Zuo, J.-L.; You, X.-Z. *Inorg. Chem.* **2007**, *46*, 5462. (c) Wen, H.-R.; Tang, Y.-Z.; Liu, C.-M.; Chen, J.-L.; Yu, C.-L. *Inorg. Chem.* **2009**, *48*, 10177.
- (5) Multiferroic materials are quite rare; they focus on pure inorganic compounds, with only a few belonging to molecular materials. See: (a) Cui, H.; Wang, Z.; Takahashi, K.; Okano, Y.; Kobayashi, H.; Kobayashi, A. *J. Am. Chem. Soc.* **2006**, *128*, 15074. (b) Ohkoshi, S.-i.; Tokoro, H.; Matsuda, T.; Takahashi, H.; Irie, H.; Hashimoto, K. *Angew. Chem., Int. Ed.* **2007**, *46*, 3238.
- (6) (a) Fang, X. K.; Anderson, T. M.; Hill, C. L. *Angew. Chem., Int. Ed.* **2005**, *44*, 3540. (b) Xin, F. B.; Pope, M. T. *J. Am. Chem. Soc.* **1996**, *118*, 7731. (c) Zhang, Z.-M.; Li, Y.-G.; Yao, S.; Wang, E.-B.; Wang, Y.-H.; Clérac, R. *Angew. Chem., Int. Ed.* **2009**, *48*, 1581. (d) Kong, X.-J.; Wu, Y.; Long, L.-S.; Zheng, L.-S.; Zheng, Z. *J. Am. Chem. Soc.* **2009**, *131*, 6919.
- (7) (a) Aromí, G.; Claude, J. P.; Knapp, M. J.; Huffman, J. C.; Hendrickson, D. N.; Christou, G. *J. Am. Chem. Soc.* **1998**, *120*, 2977. (b) Aromí, G.; Knapp, M. J.; Claude, J. P.; Huffman, J. C.; Hendrickson, D. N.; Christou, G. *J. Am. Chem. Soc.* **1999**, *121*, 5489.
- (8) Manoli, M.; Collins, A.; Parsons, S.; Candini, A.; Evangelisti, M.; Brechin, E. K. *J. Am. Chem. Soc.* **2008**, *130*, 11129.
- (9) (a) McKee, V.; Tandon, S. S. *J. Chem. Soc., Chem. Commun.* **1988**, 1334. (b) Mikuriya, M.; Hashimoto, Y.; Kawamori, A. *Chem. Lett.* **1995**, *24*, 1095. (c) Lan, Y.; Novitchi, G.; Clerac, R.; Tang, J.-K.; Madhu, N. T.; Hewitt, I. J.; Anson, C. E.; Brooker, S.; Powell, A. K. *Dalton Trans.* **2009**, 1721. (d) Afrati, T.; Dendrinou-Samara, C.; Raptopoulou, C. P.; Terzis, A.; Tangoulis, V.; Kessissoglou, D. P. *Angew. Chem., Int. Ed.* **2002**, *41*, 2148.
- (10) Shores, M. P.; Sokol, J. J.; Long, J. R. *J. Am. Chem. Soc.* **2002**, *124*, 2279.
- (11) (a) Okubo, T.; Kawajiri, R.; Mitani, T.; Shimoda, T. *J. Am. Chem. Soc.* **2005**, *127*, 17598. (b) Lu, Y. Y.; Claud, J.; Neese, B.; Zhang, Q. M.; Wang, Q. *J. Am. Chem. Soc.* **2006**, *128*, 8120. (c) Ye, Q.; Wang, X.-S.; Zhao, H.; Xiong, R.-G. *Chem. Soc. Rev.* **2005**, *34*, 208. (d) Zhang, W.; Xiong, R.-G.; Huang, S. D. *J. Am. Chem. Soc.* **2008**, *130*, 10468. (e) Ye, H.-Y.; Fu, D.-W.; Zhang, Y.; Zhang, W.; Xiong, R.-G.; Huang, S. D. *J. Am. Chem. Soc.* **2009**, *131*, 42. (f) Li, X.-L.; Chen, K.; Liu, Y.; Wang, Z.-X.; Wang, T.-W.; Zuo, J.-L.; Li, Y.-Z.; Wang, Y.; Zhu, J. S.; Liu, J.-M.; Song, Y.; You, X.-Z. *Angew. Chem., Int. Ed.* **2007**, *46*, 6820.

JA910310P